Theoretical Study of the Asymmetric Conjugate Alkenylation of Enones Catalyzed by Binaphthols

ARTICLE *in* THE JOURNAL OF ORGANIC CHEMISTRY · AUGUST 2008

Impact Factor: 4.72 · DOI: 10.1021/jo8007463 · Source: PubMed

3 AUTHORS:

Robert S Paton
University of Oxford
68 PUBLICATIONS **1,051** CITATIONS
SEE PROFILE

Jonathan M Goodman
University of Cambridge
218 PUBLICATIONS **4,098** CITATIONS
SEE PROFILE

Silvina Pellegrinet
National University of Rosario, Argentina (…
40 PUBLICATIONS **394** CITATIONS
SEE PROFILE

JOC Article

Theoretical Study of the Asymmetric Conjugate Alkenylation of Enones Catalyzed by Binaphthols

Robert S. Paton,[†] Jonathan M. Goodman,*[,†] and Silvina C. Pellegrinet*[,‡]

Unilever Centre for Molecular Science Informatics, Department of Chemistry, University of Cambridge, Lensfield Road, Cambridge CB2 1EW, United Kingdom, and Instituto de Química Rosario (CONICET), Facultad de Ciencias Bioquímicas y Farmacéuticas, Universidad Nacional de Rosario, Suipacha 531, Rosario (2000), Argentina

jmg11@cam.ac.uk; pellegrinet@iquios.gov.ar

Received April 3, 2008

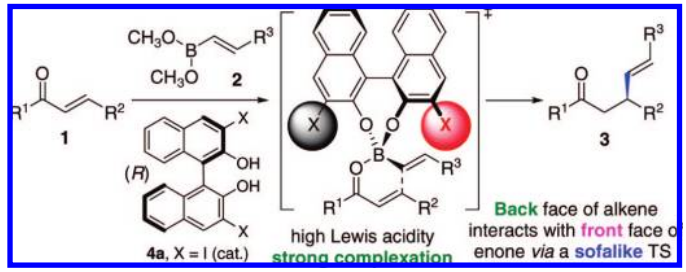

To rationalize the experimental results observed in the asymmetric conjugate addition of alkenylboronates to enones catalyzed by binaphthols and shed light into the factors controlling the rate, the selectivity, and the substituent effects of this process, a theoretical DFT study has been performed. The calculations suggest the catalytic cycle is finely balanced. Reversible exchange of methoxy ligands gives rise to the binaphthol-derived alkenylboronate, which is highly Lewis acidic and strongly coordinates to the enone carbonyl in a reversible fashion, lowering the energy barrier for the subsequent conjugate addition step. The key asymmetric step goes through a sofalike transition structure in which the boron atom is strongly bound to the carbonyl oxygen and lies in the plane of the enone moiety. A steric clash between one of the iodine atoms of the ligand and one face of the enone seems to be responsible for the facial discrimination. The alternative reaction channel in which only one methoxy ligand of the alkenylboronate is exchanged was investigated too and was computed to be disfavored. The [4 + 2] and the [4 + 3] pathways for the competitive hetero-Diels−Alder reaction were also found to be disfavored relative to the conjugate alkenylboration. In addition, the effects of substitution on the enone and the alkenylboronate have been evaluated. Calculations correctly reproduced the experimental reactivity trends and enantiomeric ratios.

Introduction

The development of highly efficient catalytic asymmetric reactions is currently one of the most challenging tasks for organic chemists. The literature has witnessed a remarkable increase of activity in this field over the last years. As a result, a number of important new methodologies for performing different chemical transformations have been described. Nevertheless, mechanistic uncertainties about catalytic cycles sometimes make it difficult to optimize the reactions and to design new catalysts rationally. Therefore, the study of the mechanisms that operate in these processes is vital for the development of new reactions and innovative concepts in catalysis.

In the past decade, Chong and co-workers investigated a number of stoichiometric reactions of 3,3′-disubstituted binaphthol organoboronates. These include the asymmetric conjugate addition of alkynylboronates to enones[1] and the asymmetric allylboration of aldehydes and ketones[2] and of cyclic imines.[3] In 2005, they described the conjugate addition of *B*-1-alkynyldiisopropylboronates to enones catalyzed by 3,3′-disubstituted binaphthols, providing a major improvement to the stoichio-

[†] University of Cambridge.
[‡] CONICET, Universidad Nacional de Rosario. Phone/fax: +54 341 4370477.

(1) Chong, J. M.; Shen, L.; Taylor, N. J. *J. Am. Chem. Soc.* **2000**, *122*, 1822–1823.
(2) Wu, T. R.; Shen, L.; Chong, J. M. *Org. Lett.* **2004**, *6*, 2701–2704.
(3) Wu, T. R.; Chong, J. M. *Org. Lett.* **2006**, *8*, 15–18.

10.1021/jo8007463 CCC: $40.75
Published on Web 06/11/2008

SCHEME 1. Catalytic Asymmetric Conjugate Alkenylboration of Enones

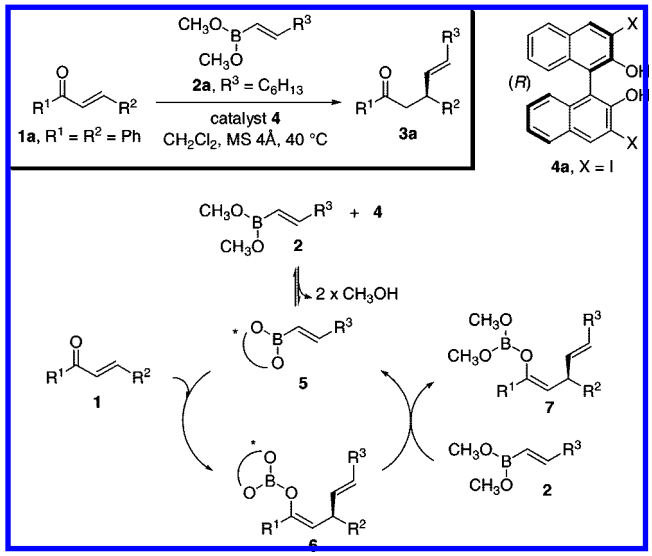

metric procedure in terms of preparative simplicity and economy of chiral material.[4] Moreover, this outstanding contribution proved that catalytic amounts of binaphthol ligands could be used to accelerate the reactions of boronates efficiently and also to achieve high levels of stereoselectivity. Since then, this ligand-accelerated protocol has been applied to the catalytic asymmetric allylboration of ketones[5] and acyl amines[6] and to the catalytic asymmetric conjugate alkenylboration[7] of enones.

Experimental results for the study of the 1,4-alkenylboration of chalcone (**1a**, Scheme 1) with alkenylboronate **2a** showed that the best results were obtained when the binaphthol had electron-withdrawing groups such as iodine atoms in the 3 and 3′ positions (**4a**). Also, no product was obtained in the absence of binaphthols or with the addition of alkyl diols such as diisopropyl tartrate. Furthermore, the addition of water or methanol inhibited the reaction.

The mechanism proposed by Wu and Chong for the catalytic asymmetric conjugate addition of alkenylboronates to enones is depicted in Scheme 1.[7] Transesterification of **2** with catalyst **4** affords the chiral binaphthol-derived alkenylboronate **5**, which then adds to the enone in a conjugate fashion, yielding intermediate **6**. Exchange of ligands simultaneously regenerates the chiral reagent **5**, giving dimethoxyboron enolate **7**. Protonation of **7** during workup generates the β-alkenyl ketone product **3**. High selectivities were obtained for enones having aryl or alkyl groups in the β position and also for conjugated dienones. Six-membered chairlike transition states were proposed to explain the observed stereoselectivities (Figure 1). One of the possible transition structures was suggested to be destabilized by a steric interaction of the pseudoequatorial alkenyl group with the binaphthol.

Previous theoretical investigations from our group provided a rationale to explain the catalysis exerted by binaphthols in the conjugate alkynylboration of enones.[8] We have now

(4) Wu, T. R.; Chong, J. M. *J. Am. Chem. Soc.* **2005**, *127*, 3244–3245.
(5) Lou, S.; Moquist, P. N.; Schaus, S. E. *J. Am. Chem. Soc.* **2006**, *128*, 12660–12661.
(6) Lou, S.; Moquist, P. N.; Schaus, S. E. *J. Am. Chem. Soc.* **2007**, *129*, 15398–15404.
(7) Wu, T. R.; Chong, J. M. *J. Am. Chem. Soc.* **2007**, *129*, 4908–4909.
(8) Pellegrinet, S. C.; Goodman, J. M. *J. Am. Chem. Soc.* **2006**, *128*, 3116–3117.

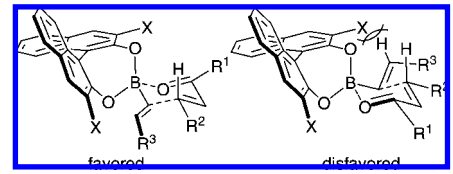

FIGURE 1. Six-membered chairlike transition states proposed for the 1,4-alkenylboration.

performed a theoretical DFT study to rationalize the experimental results observed in the catalytic asymmetric conjugate addition of alkenylboronates to enones and to shed light into the mechanism, the factors controlling the rate, the selectivity, and the substituent effects of this process.

Computational Methods

All calculations were performed with either Gaussian 03[9] or Jaguar version 6.5.[10] Density functional theory (DFT) calculations were carried out with the B3LYP functional.[11] For Gaussian calculations, the 6-31G*[12] basis set was used for all atoms except for iodine, which was described by the LANL2DZ[13] effective core potential of Hay and Wadt (6-31G* + LANL2DZ denoted as 631LAN). For Jaguar, the equivalent lacvp* basis set was used unless otherwise noted. The choice of this level of theory for the present investigation was based on our previous experience on the studies of reactions of organoboranes,[8,14] which are in good agreement with experimental results. Geometries for all structures were fully optimized and frequency calculations were used to confirm the nature of the stationary points. All transition structures were confirmed to have only one imaginary frequency corresponding to the formation of the expected bonds. Intrinsic Reaction Coordinate (IRC) or Quick Reaction Coordinate (QRC)[15] calculations were performed to determine the connections between stationary points. To analyze the formation and breaking of bonds, Wiberg bond indices (WBIs) were calculated by using the Natural Bond Orbital (NBO) program[16,17] as implemented in Gaussian 03. Reported thermochemical properties include zero-point energies (ZPEs) without scaling and were calculated at 1 atm and 298.15 K. Free energies in solution were computed on the structures optimized in the gas phase with the Polarizable Continuum Model (PCM) as implemented in Gaussian 03 with dichloromethane as the solvent.[18]

CHART 1

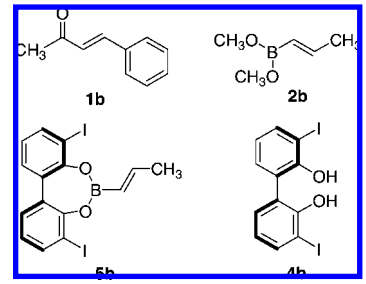

Results and Discussion

Study of the Reaction Mechanism and Rationalization of the Stereoselectivity. To begin our study, we first investigated the reaction using enone **1b**, alkenylboronates **2b** and **5b** as models for **2a** and **5a** respectively ($R^3 = C_6H_{13}$, X = I, Scheme 1), and 3,3′-diiodo-1,1′-biphenyl-2,2′-diol (**4b**) as a model for 3,3′-diiodobinaphthol (**4a**) (Chart 1).

We first located the transition structures (TSs) corresponding to the conjugate addition of alkenylboronates **2b** and **5b** to enone **1b**. Unlike the 1,4-alkynylboration, in which there is only one

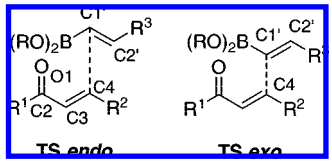

FIGURE 2. Possible modes of attack for the 1,4-alkenylboration.

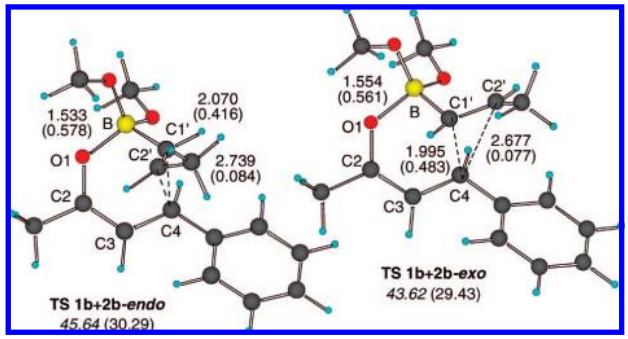

FIGURE 3. Optimized geometries for the transition structures of the 1,4-alkenylboration of **1b** with **2b** with selected distances (in Å) and WBIs (in parentheses). Free energies relative to reactants in the gas phase (in italics) and in solution (in parentheses) are also shown (in kcal mol^{-1}).

transition structure for the attack of the linear alkynylboronate to the enone, conformers arising from rotation around the B−C1′ bond had to be considered (Figure 2). We use the following nomenclature for the two possible modes of attack: the TS in which C2′ is close to the π system of the enone is called "TS *endo*" and the TS in which C2′ is away from the π system of the enone is called "TS *exo*". Therefore, for the achiral alkenylboronates such as **2b** there are two possible TSs for the conjugate addition (*endo*/*exo*), while for the chiral derivatives such as **5b** there are four TSs (*endo*/*exo* for each face of the enone, *Re*/*Si*).

Figure 3 shows the transition structures corresponding to the 1,4-addition of alkenylboronate **2b** to enone **1b**. Both structures present similar C1′−C4 and C2′−C4 distances (∼2.0 and 2.7 Å, respectively) and the boron atom is coordinated to the oxygen of the enone carbonyl (B−O1 distances ∼1.5 Å). However, the hydrogen attached to C1′ and the methyl on C2′ lie closer to the phenyl ring in **TS 1b+2b-*endo***, which might explain the higher energy relative to **TS 1b+2b-*exo***. It is interesting to point out that atoms B, O1, C2, C3, and C4 are roughly in the same plane, as might be expected given the sp^2 hybridization of the atoms of the enone moiety, which suggests that these are sofalike transition structures, and not the chairlike structures proposed by Wu and Chong.[7]

SCHEME 2. Reaction Coordinate for the 1,4-Alkenylboration of 1b with 2b Corresponding to TS 1b+2b-*exo* and Free Energies in Dichloromethane

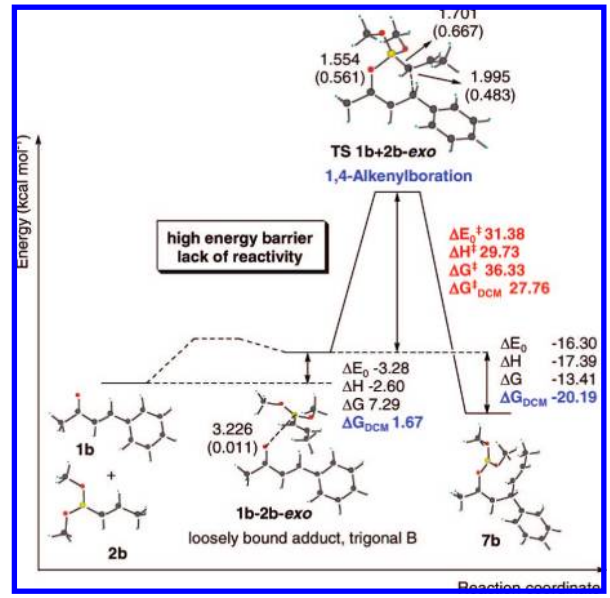

The transition structures located for the conjugate addition of alkenylboronate **5b** to enone **1b** are depicted in Figure 4. Again, the boron atom is strongly bound to the oxygen and lies in the plane of the enone moiety in all transition structures. Inspection of the geometries also reveals that transition structures for **5b** have comparable B−O1, C1′−C4, and C2′−C4 distances and that these are slightly shorter than those corresponding to the dimethyl analogue **2b** (Figure 3). Furthermore, computed WBIs are higher, indicating stronger bonding interactions for the TSs corresponding to alkenylboronate **5b**. In addition, the *exo* preference is maintained for the attack to both faces of the enone and **TS 1b+5b-*Re-exo*** was calculated to be favored over **TS 1b+5b-*Si-exo*** by 2.56 kcal mol^{-1} (4.26 kcal mol^{-1} in solution). Interestingly, the reaction pathways for the chiral alkenylboronate **5b** showed considerably lower free energy barriers than those for **2b**, by more than 10 kcal mol^{-1} both in the gas phase and in solution.

We then examined the reaction coordinates for the conjugate addition of alkenylboronates **2b** and **5b** to enone **1b** by performing IRC calculations starting from the transition structures. Scheme 2 shows the reaction coordinate for the 1,4-alkenylboration of **1b** with **2b** corresponding to the more stable transition structure **TS 1b+2b-*exo***. The transition structures for the reaction of dimethyl alkenylboronate **2b** were found to be connected to loosely bound molecular complexes (**1b−2b-*endo*** and ***-exo***), in which the boron atom remains trigonal and is ∼3.2 Å from the carbonyl oxygen of the enone, suggesting that when reactants approach they experience a weak stabilizing interaction (for all structures see the Supporting Information). The calculated B−O1 Wiberg bond indices for complexes **1b−2b-*endo*** and ***-exo*** were very low (0.008 and 0.011, respectively). Although the enthalpic contribution of this interaction is

(9) Frisch, M. J.; et al. *Gaussian 03*, Revision C.02; Gaussian Inc.: Wallingford, CT, 2004.
(10) *Jaguar*, version 6.5; Schrodinger LLC: New York, 2005.
(11) (a) Becke, A. D. *J. Chem. Phys.* **1993**, *98*, 5648–5652. (b) Lee, C. T.; Yang, W. T.; Parr, R. G. *Phys. Rev. B* **1988**, *37*, 785–789.
(12) Hehre, W. J.; Radom, L.; Schleyer, P. v. R.; Pople, J. A. *Ab Initio Molecular Orbital Theory*; Wiley: New York, 1986.
(13) Hay, P. J.; Wadt, W. R. *J. Chem. Phys.* **1985**, *82*, 299–310.
(14) For example see:(a) Pellegrinet, S. C.; Silva, M. A.; Goodman, J. M. *J. Am. Chem. Soc.* **2001**, *123*, 8832–8837. (b) Silva, M. A.; Pellegrinet, S. C.; Goodman, J. M. *J. Org. Chem.* **2002**, *67*, 8203–8209. (c) Silva, M. A.; Pellegrinet, S. C.; Goodman, J. M. *J. Org. Chem.* **2003**, *68*, 4059–4066. (d) Silva, M. A.; Pellegrinet, S. C.; Goodman, J. M. *Arkivoc* **2003**, *10*, 556–565.
(15) (a) Silva, M. A.; Goodman, J. M. *Tetrahedron Lett.* **2003**, *44*, 8233–8236. (b) Silva, M. A.; Goodman, J. M. *Tetrahedron Lett.* **2005**, *46*, 2067–2069.
(16) (a) Reed, A. E.; Weinstock, R. B.; Weinhold, F. *J. Chem. Phys.* **1985**, *83*, 735–746. (b) Reed, A. E.; Curtiss, L. A.; Weinhold, F. *Chem. Rev.* **1988**, *88*, 899–926.
(17) *NBO*, Version 3.1; Glendening, E. D., Reed, A. E., Carpenter, J. E., Weinhold, F.
(18) (a) Miertus, S.; Scrocco, E.; Tomasi, J. *J. Chem. Phys.* **1981**, *55*, 117–129. (b) Mennucci, B.; Tomasi, J. *J. Chem. Phys.* **1997**, *106*, 5151–5158.
(19) We were unable to locate the TSs for the formation of complexes **1b−2b**.

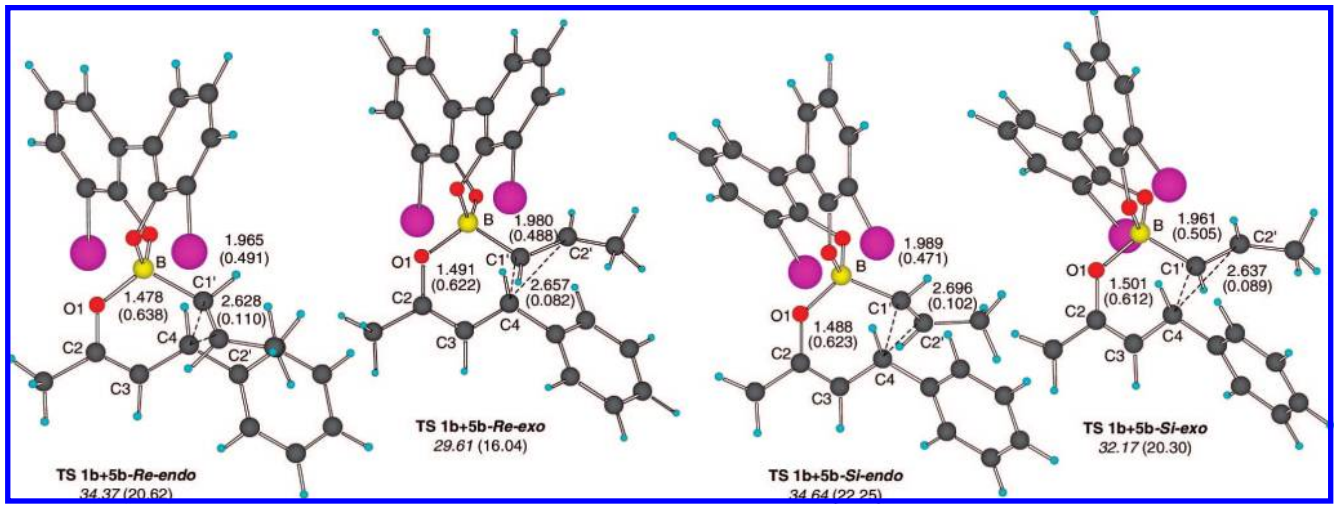

FIGURE 4. Optimized geometries for the transition structures of the 1,4-alkenylboration of **1b** with **5b** with selected distances (in Å) and WBIs (in parentheses). Free energies relative to reactants in the gas phase (in italics) and in solution (in parentheses) are also shown (in kcal mol^{-1}).

SCHEME 3. Reaction Coordinate for the 1,4-Alkenylboration of 1b with 5b Corresponding to TS 1b+5b-*Re-exo* and Free Energies in Dichloromethane

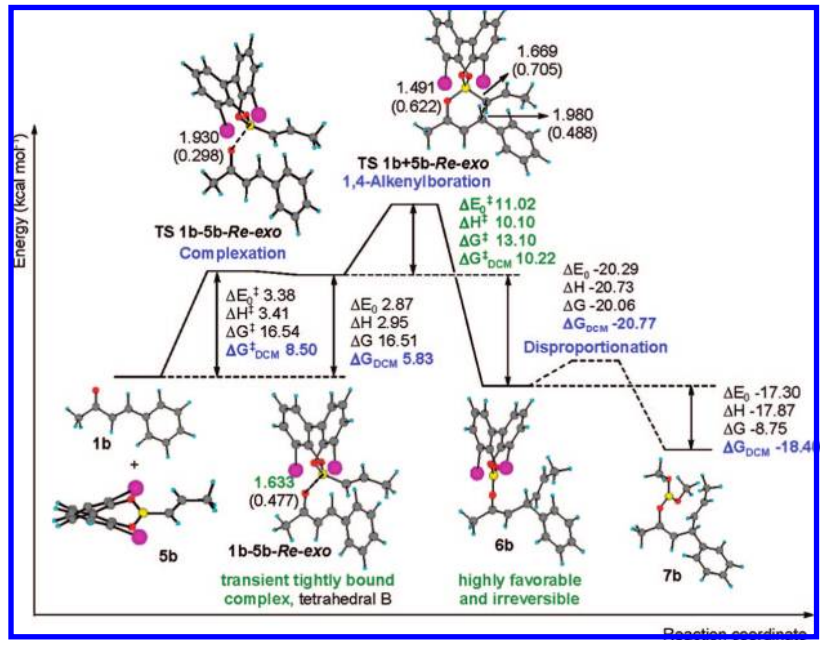

favorable (−1.12 and −2.60 kcal mol^{-1} relative to reactants for **1b**−**2b**-***endo*** and ***-exo***, respectively), the approach of the reagents results in a loss of entropy, raising the reaction free energy to 9.11 and 7.29 kcal mol^{-1}.[19] The activation free energies for the conjugate addition step were computed to be considerably higher (36.52 and 36.33 kcal mol^{-1}), which reflects the lack of reactivity of the methyl-derived alkenylboronate. The transition structures were also shown to be connected to the 1,4-alkenylboration products, which showed lower energies than the reactants, suggesting that the C−C bond-formation reaction is thermodynamically favorable (Scheme 2).

Stabilization of the charged species by solvation was observed with the inclusion of solvent effects (dichloromethane). The calculation of energies in solution suggests the molecular complex has essentially the same energy as the reactants. Also, the activation free energy for the conjugate addition decreases whereas the reaction free energy increases, making this step more favorable. However, the energy barrier corresponding to **TS 1b**+**2b-*exo*** is still considerable (27.76 kcal mol^{-1}).

IRC calculations for the four transition structures of the conjugate addition of the chiral analogue **5b** were also performed. Scheme 3 shows the reaction coordinate for the 1,4-alkenylboration of **1b** with **5b** corresponding to the more stable transition structure **TS 1b**+**5b-*Re-exo***. In line with our previous results for the analogous alkynylboration, the transition structures were shown to be connected to coordination complexes in which the B−O1 distances are considerably shorter and the boron atom is more tetrahedral than in **1b**−**2b-*endo*** and ***-exo*** (see the Supporting Information). The calculated boron−oxygen WBIs confirm that the reactants experience a strong B−O1 interaction. For example, in **1b**−**5b-*Re-exo*** the B−O1 distance is 1.633 Å and the WBI is 0.477. This suggests the boron atom of alkenylboronate **5b** effectively coordinates to the enone carbonyl forming a tightly bound complex. Once complex **1b**−**5b-*Re-***

SCHEME 4. Catalytic Cycle for the 1,4-Alkenylboration of Enone 1b

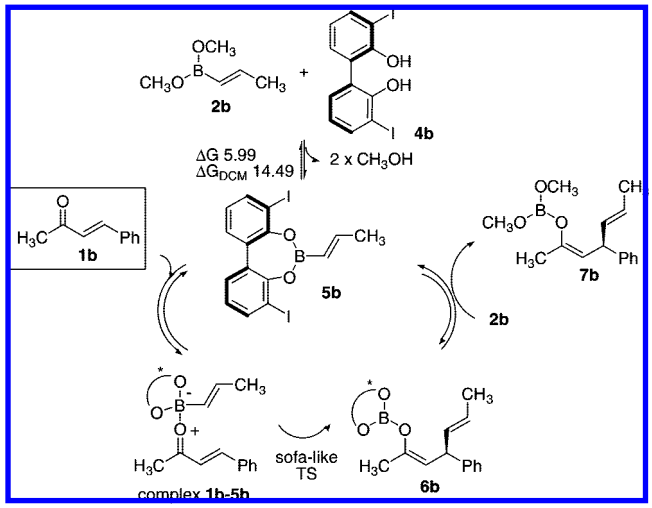

exo is formed, the activation free energy of the conjugate addition is significantly reduced (13.10 kcal mol^{-1}). The generation of the 1,4-alkenylboration product is highly favorable ($-$20.06 kcal mol^{-1}), in part because most of the entropy is lost when the reagents combine to form the complex. As a result, the conjugate addition step is predicted to be irreversible since the free energy barrier for going back to complex **1b**$-$**5b-*Re-exo*** is so high (33.16 kcal mol^{-1}).

Unlike the reaction coordinate of the dimethyl alkenylboronate **2b**, we were able to locate the transition structure for the formation of complex **1b**$-$**5b-*Re-exo*** in this case. Transition structure **TS 1b**$-$**5b-*Re-exo*** has almost the same free energy as the complex, despite the fact that the B$-$O1 distance is 0.3 Å longer and has a WBI of 0.298. The reaction coordinate reveals that complex **1b**$-$**5b-*Re-exo*** should be present at a very low concentration since complexation is highly reversible and the 1,4-alkenylboration is very fast and irreversible. As a consequence, the complexes can be considered as transient species that are present at very low concentrations, and so the activation energies calculated from the separate reactants can be used to compute approximate ratios. Due to the complexity of the disproportionation step, no attempts were made to study the reaction coordinate from **6b** to **7b** in further detail. However, the overall free energy change calculated for this transformation is $-$8.75 kcal mol^{-1}, suggesting that the exchange of ligands favors the formation of the dimethoxyboron enolate **7b**. This is one of the conditions that must be met so that the chiral alkenylboronate **5b** can be regenerated.

Free energies in solution, computed for the geometries optimized in the gas phase, give lower energy barriers for both complexation and 1,4-alkenylboration. This also makes each step more thermodynamically favorable.

IRCs depicted in Schemes 2 and 3 also suggest that the formation of B$-$O1 and C1′$-$C4 σ bonds occurs in a concerted fashion with the breaking of the B$-$C1′ bond and the reorganization of the π electrons in the enone system. However, transition structures are shown to be asynchronous since B$-$O1 bond formation is more advanced than C1′$-$C4 bond formation, which, in turn, is more advanced than B$-$C1′ bond breaking. For example, in **TS 1b**+**2b-*exo*** WBIs are 0.561, 0.483, and 0.667 respectively, while the corresponding values in **TS 1b**+**5b-*Re-exo*** are 0.622, 0.488, and 0.705.

On the basis of the results of our calculations, we propose the catalytic cycle depicted in Scheme 4 for the 1,4-alkenylboration of enone **1b**. This differs from the Chong proposal because it includes the transient complex **1b**$-$**5b**, and the key asymmetric step goes through a sofalike and not a chairlike transition state.

To rationalize the different reactivity of alkenylboronates **2b** and **5b**, we have studied the frontier molecular orbitals of the reagents and the complexes (Figure 5). The most important interaction between enone **1b** and the dimethyl alkenylboronate **2b** is a typical interaction for a nucleophilic addition, i.e., that between the LUMO of the enone and the HOMO of the alkenylboronate (energy gap 4.785 eV). Alkenylboronate **5b** has lower energy FMOs (HOMO-3 and LUMO) so these orbitals interact with the LUMO and the HOMO of enone **1b** with energy gaps of 5.199 and 5.023 eV, respectively. The HOMO$_{\text{enone}\,\mathbf{1b}}$/LUMO$_{\text{alkenylboronate}\,\mathbf{5b}}$ interaction gives rise to the formation of coordination complex **1b**$-$**5b-*Re-exo***, which has a higher energy HOMO-3 and a lower energy LUMO and, consequently, experiences a very favorable intramolecular HOMO-3/LUMO interaction of 3.333 eV. On the other hand, molecular complex **1b**$-$**2b-*exo*** shows a weaker intramolecular HOMO-1/LUMO interaction of 4.626 eV, similar to the one computed in the parent reagents.

Inspection of the optimized geometries of boronate analogues **2b** and **5b** reveals that C$-$O$-$B$-$C1′ torsion angles are either 0° or 180° in **2b** and close to 145° in **5b**. This suggests that in the binaphthol-derived alkenylboronate the oxygens might be less able to donate electron density to the boron atom. Delocalization of the oxygen lone pairs into the adjacent aromatic system, which is reinforced by the presence of the electron-withdrawing iodine atoms in the 3 and 3′ positions, further enhances the Lewis acid character of the boron and considerably lowers the energy of the LUMO of **5b**. Calculated boron$-$oxygen WBIs confirm this idea, because they are 0.900 and 0.911 in **2b** and 0.821 and 0.830 in **5b**.

The enantiomeric ratio computed for the conjugate alkenylboration reaction of enone **1b** (98.6:1.4) is in excellent agreement with the experimental value obtained with alkenylboronate **2a** and catalyst **4a** (Scheme 1) (99.1:0.9).[20] This supports the choice of the B3LYP/631LAN method and also of 3,3′-diiodo-1,1′-biphenyl-2,2′-diol (**4b**) as a model for 3,3′-diiodobinaphthol (**4a**). The enantiomeric ratio calculated from free energies in solution is higher (99.9:0.1) but also reproduces the excellent facial selectivity observed in the reaction. Transition structures **TS 1b**+**5b-*Re-exo*** and **TS 1b**+**5b-*Si-exo*** show very similar electronic interactions since B$-$O1, C1′$-$C4, and C2′$-$C4 WBIs are nearly the same (Figure 4). Therefore, the destabilization of the latter needs to be explained in terms of steric interactions. In **TS 1b**+**5b-*Si-exo*** one of the iodine atoms of the chiral ligand is flanked by the alkenyl group and the β-substituents of the enone, which results in three hydrogen$-$iodine close contacts (Figure 6). The distances between these atoms are close to the sum of the van der Waals radii of hydrogen (1.20 Å) and iodine (1.98 Å). In contrast, in **TS 1b**+**5b-*Re-exo*** the ligand is almost perpendicular to the plane of the enone, so steric clashes are avoided.

The facial selectivity of the 1,4-alkenylboration can be summarized as depicted in Scheme 5. The sofalike transition

(20) Ratios were computed by using Boltzmann factors based on activation free energies and are of qualitative value. Calculations demonstrated that the *endo* transition structures contribute to the ratio by less than 0.1%.

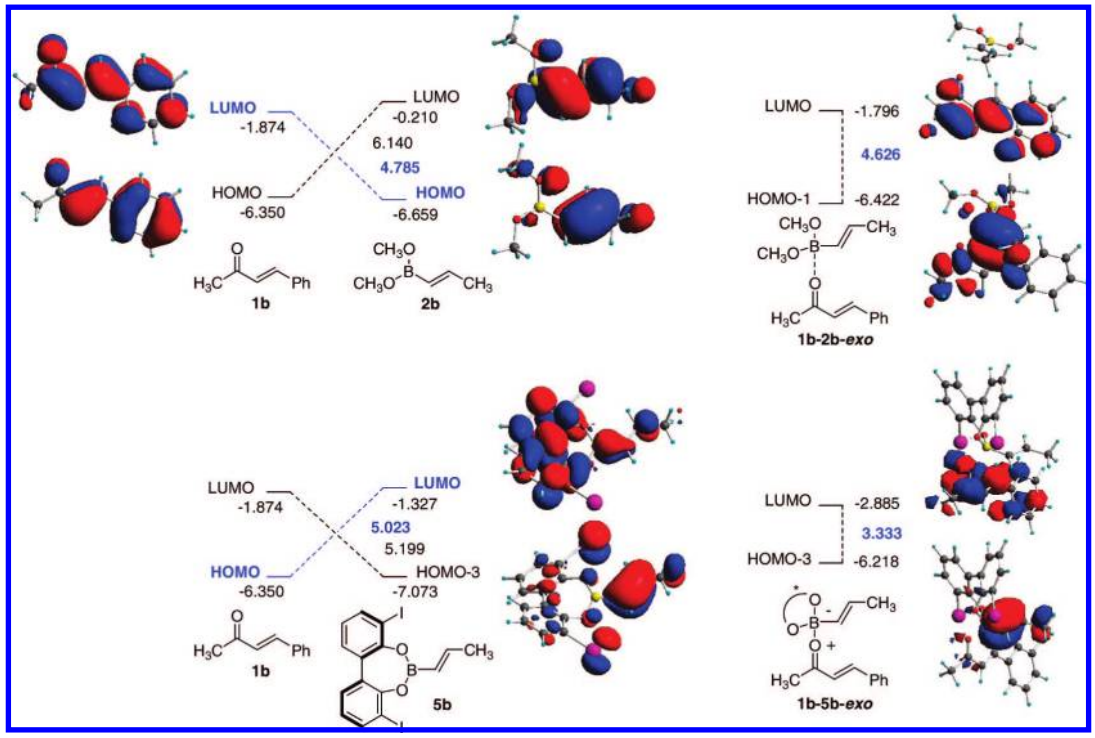

FIGURE 5. FMO interactions between enone **1b** and alkenylboronates **2b** and **5b**. Molecular orbital energies and energy gaps are shown in eV.

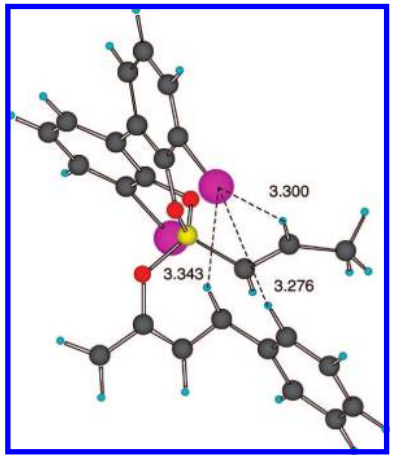

FIGURE 6. Close contacts observed in **TS 1b**+**5b**-***Si-exo*** (in Å).

SCHEME 5. Facial Selectivity of the 1,4-Alkenylboration

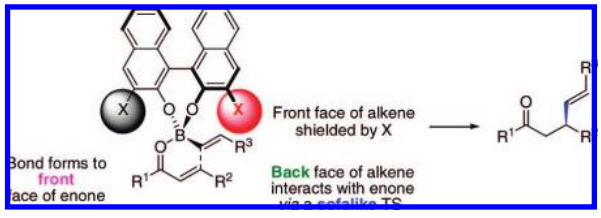

structure, which has five atoms of the six-membered ring in the same plane, ensures that the new bond is either from the back face of the alkene to the front face of the enone (as in **TS 1b**+**5b**-***Re-exo***) or from the front face of the alkene to the back face of the enone (as in **TS 1b**+**5b**-***Si-exo***). The front face of the alkene is shielded by the electron-withdrawing group X, and this precludes the attack to the back face of the enone. This cartoon, which is based on the calculated geometries of the

SCHEME 6. Exchange of Ligands of Alkenylboronate 2b with 4b and Free Energy Changes (in kcal mol^{-1})

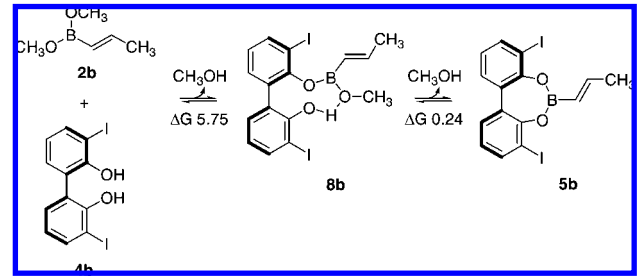

transition structures, can be used as a mnemonic for rationalizing and predicting the selectivity in these reactions.[21]

Study of Competitive Pathways. We have also investigated the alternative reaction channel in which only one methoxy ligand of the alkenylboronate is exchanged. Schaus and co-workers proposed such a mechanism for the asymmetric addition

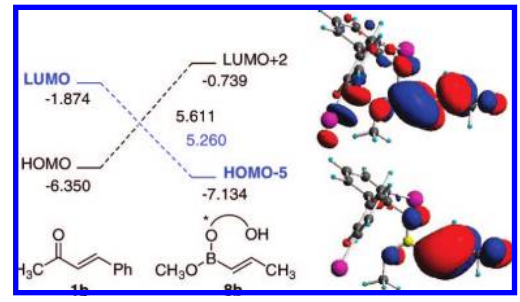

FIGURE 7. FMO interactions between enone **1b** and alkenylboronate **8b**. Molecular orbital energies and energy gaps are shown in eV.

of allyldiisopropoxyboronates to ketones and acyl imines catalyzed by binaphthols.[5,6] They suggested that the allylboronate resulting from the exchange of one isopropoxy group is

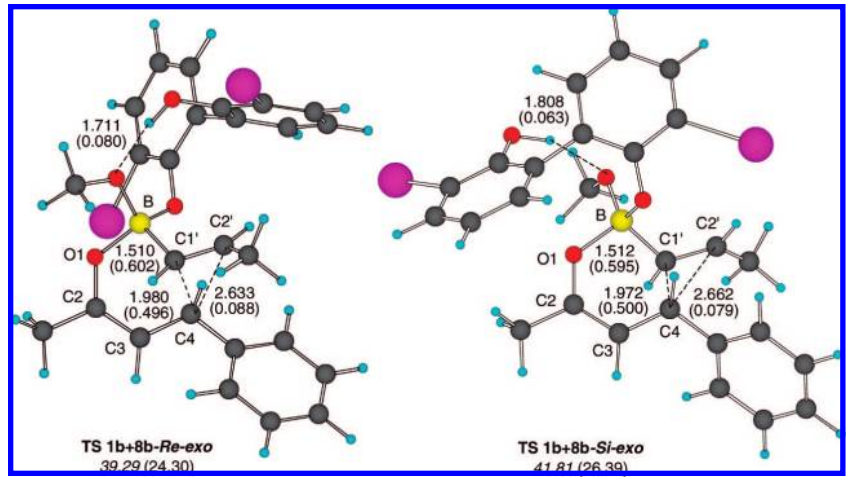

FIGURE 8. Optimized geometries for the transition structures of the 1,4-alkenylboration of **1b** with **8b** with selected distances (in Å) and WBIs (in parentheses). Free energies from reactants in the gas phase (in italics) and in solution (in parentheses) are also shown (in kcal mol^{-1}).

activated by hydrogen bonding between the remaining hydroxyl in the binaphthol and the isopropoxy group attached to the boron. To consider this possibility, we studied the equivalent mechanism for the 1,4-alkenylboration reaction (Scheme 6). Formation of alkenylboronate **8b** by exchange of one of the methoxy groups of **2b** seems to be disfavored by 5.75 kcal mol^{-1}. In addition, the reaction free energy for the second exchange of ligands was computed to be 0.24 kcal mol^{-1}. It may be, therefore, that alkenylboronates **8b** and **5b** are present at very low concentrations.

Figure 7 shows the FMO interactions between enone **1b** and alkenylboronate **8b**. As for alkenylboronate **2b**, in this case the $HOMO\text{-}5_{alkenylboronate\,8b}/LUMO_{enone\,1b}$ is the major interaction but, since the HOMO-5 has a lower energy, the energy gap is larger (5.260 eV), indicating that **8b** should be less nucleophilic than **2b**. In addition, the LUMO+2 has an energy between those of **2b** and **5b**, which suggests that alkenylboronate **8b** is more electrophilic than **2b** and less electrophilic than **5b**. Computed C−O−B−C1′ torsion angles for alkenylboronate **8b** are either 0° or 180°, similar to those in **2b**, and boron−oxygen WBIs are 0.880 and 0.835. This suggests that the oxygens in **8b** have an ability to donate electron density to the boron atom between those of **2b** and **5b**.

The *exo* transition structures found for the 1,4-alkenylboration of enone **1b** with alkenylboronate **8b** are shown in Figure 8.[22] The B−O1, C1′−C4, and C2′−C4 distances in both structures are similar to those corresponding to the transition structures for **5b** (∼1.5, 2.0, and 2.7 Å, respectively) and the same is observed for the WBIs. Once more, the boron atom is strongly coordinated to the carbonyl and lies in the plane of the enone system. Also, hydrogen bonding seems to be stronger in the transition structures than in the starting alkenylboronate since the hydrogen−oxygen distance in **8b** is 1.974 Å and the corresponding WBI is 0.034. As for alkenylboronate **5b**, the transition structure corresponding to the attack of the *Re* face (**TS 1b+8b-*Re-exo***) was favored over its *Si* counterpart (**TS 1b+8b-*Si-exo***) by 2.52 kcal mol^{-1} (2.09 kcal mol^{-1} in solution)

SCHEME 7. Hetero-Diels−Alder Reaction between Enone 1b and Alkenylboronates 2b and 5b

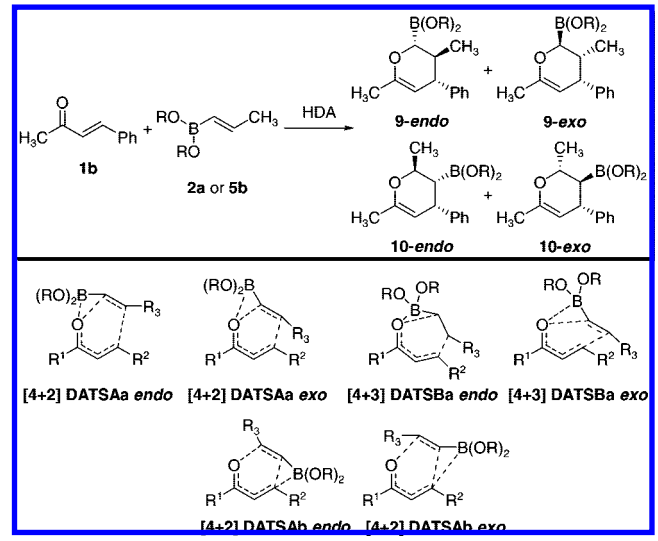

due to steric reasons. In addition, the free energies calculated from reactants for both transition structures are between those obtained for analogues **2b** and **5b**. This suggests that exchange of only one methoxy ligand gives an alkenylboronate that is more reactive than **2b** but less reactive than **5b** and, given the ease of formation of **5b** from **8b** via loss of methanol, the proposed alternative pathway for the 1,4-alkenylboration reaction involving **8b** should be disfavored relative to that of **5b**.

We then studied the [4 + 2] and the [4 + 3] pathways for the competitive hetero-Diels−Alder (HDA) reaction between enone **1b** and alkenylboronates **2b** and **5b** (Scheme 7).[23] These reactions are related to the Diels−Alder reactions of alkenylboranes with 1,3-dienes, which have been extensively studied both experimentally[24] and theoretically.[14a,d,25] Alkenylboronates have been used in Diels−Alder reactions too, but they exhibit lower reactivity.[26] The Diels−Alder reactions of boron-activated dienophiles can occur through classical [4 + 2] TSs with [4 + 3] C−B secondary orbital interactions (DATSAs) or through nonclassical [4 + 3] TSs (DATSBs). Also, regioisomeric (**a**

(21) This scheme can also be applied to rationalize and predict the enantioselectivity of the conjugate alkynylboration of enones (see ref 4). Enantiomeric (*S*)-binaphthols were used in the conjugate alkynylboration of enones, so the bond forms to the back face of the enone.

(22) We performed conformational searches to locate the lower energy conformation for these TSs at the RHF/AM1 level of theory and then reoptimized selected structures with the B3LYP/631LAN method.

(23) For a review on boron-substituted building blocks in cycloaddition reactions see: Hilt, G.; Bolze, P. *Synthesis* **2005**, 2091–2115.

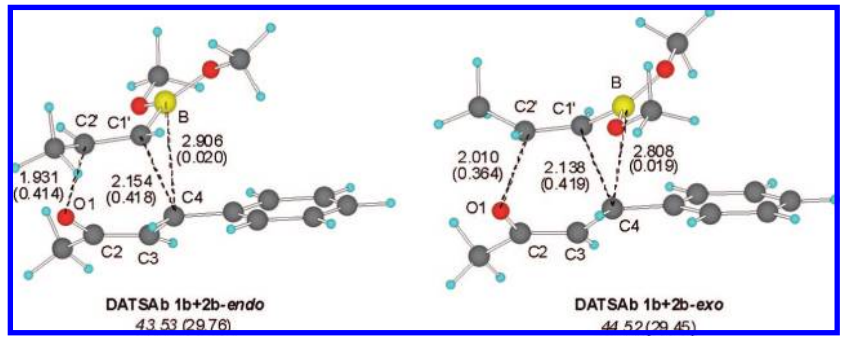

FIGURE 9. Optimized geometries for selected transition structures of the hetero-Diels−Alder reaction between **1b** and **2b** with selected distances (in Å) and WBIs (in parentheses). Free energies relative to reactants in the gas phase (in italics) and in solution (in parentheses) are also shown (in kcal mol^{-1}).

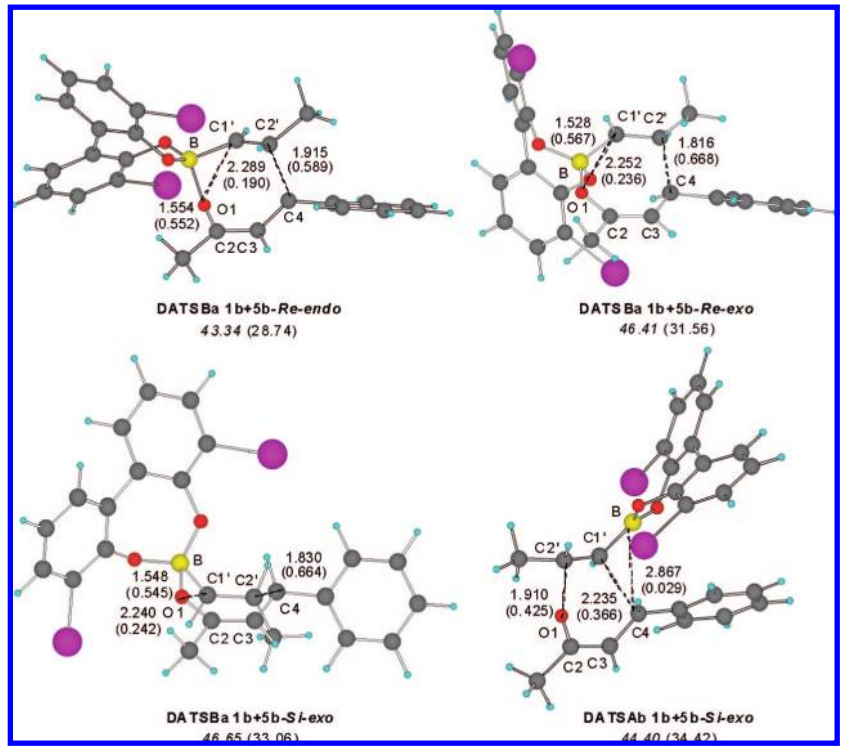

FIGURE 10. Optimized geometries for selected transition structures of the hetero-Diels−Alder reaction between **1b** and **5b** with selected distances (in Å) and WBIs (in parentheses). Free energies relative to reactants in the gas phase (in italics) and in solution (in parentheses) are also shown (in kcal mol^{-1}).

and **b**) and *endo* and *exo* diastereomeric transition structures have to be considered.

For the pathway leading to cycloadducts **9**, we have found the [4 + 2] (**DATSAa 1b+2b-*endo*** and ***-exo***) and [4 + 3] (**DATSBa 1b+2b-*endo*** and ***-exo***) transition structures for the hetero-Diels−Alder reaction between **1b** and **2b**. In addition, we have located *exo* classical TSs (**DATSAa 1b+5b-*Re-exo*** and ***-Si-exo***) and *endo* and *exo* nonclassical TSs (**DATSBa 1b+5b-*Re-*** and ***-Si***) for alkenylboronate **5b**. All attempts to locate the *endo* [4 + 2] TSs for **5b** merged in their [4 + 3] counterparts, which could be attributed to the higher electrophilic character of the boron atom of this compound. The opposite happened when we searched for the regioisomeric transition structures corresponding to products **10**, since we only found classical [4 + 2] transition structures for **2b** and **5b** (***-endo*** and ***-exo*** **DATSAb 1b+2b** and **1b+5b-*Re-*** and ***-Si***). All the transition structures are asynchronous (Figures 9 and 10, for all Diels−Alder transition structures see the Supporting Information).

(24) (a) Singleton, D. A.; Martínez, J. P. *J. Am. Chem. Soc.* **1990**, *112*, 7423–7424. (b) Singleton, D. A.; Martínez, J. P. *Tetrahedron Lett.* **1991**, *32*, 7365–7368. (c) Singleton, D. A.; Martínez, J. P.; Watson, J. V. *Tetrahedron Lett.* **1992**, *33*, 1017–1020. (d) Singleton, D. A.; Martínez, J. P.; Watson, J. V.; Ndip, G. M. *Tetrahedron* **1992**, *48*, 5831–5838. (e) Singleton, D. A.; Leung, S.-W. *J. Org. Chem.* **1992**, *57*, 4796–4797. (f) Singleton, D. A.; Martinez, J. P.; Ndip, G. M. *J. Org. Chem.* **1992**, *57*, 5768–5771. (g) Noiret, N.; Youssofi, A.; Carboni, B.; Vaultier, M. *J. Chem. Soc., Chem. Commun.* **1992**, 1105–1107. (h) Singleton, D. A.; Kim, K.; Martinez, J. P. *Tetrahedron Lett.* **1993**, *34*, 3071–3074. (i) Singleton, D. A.; Redman, A. M. *Tetrahedron Lett.* **1994**, *35*, 509–512. (j) Singleton, D. A.; Lee, Y.-K. *Tetrahedron Lett.* **1995**, *36*, 3473–3476. (k) Lee, Y.-K.; Singleton, D. A. *J. Org. Chem.* **1997**, *62*, 2255–2258. (l) Singleton, D. A.; Leung, S.-W.; Martínez, J. P.; Lee, Y.-K. *Tetrahedron Lett.* **1997**, *38*, 3163–3166. (m) Batey, R. A.; Lin, D.; Wong, A.; Hayhoe, C. L. S. *Tetrahedron Lett.* **1997**, *38*, 3699–3702. (n) Singleton, D. A.; Leung, S.-W. *J. Organomet. Chem.* **1997**, *544*, 157–161. (o) Zaidlewicz, M.; Binkul, J. R.; Sokol, W. *J. Organomet. Chem.* **1999**, *580*, 354–362.

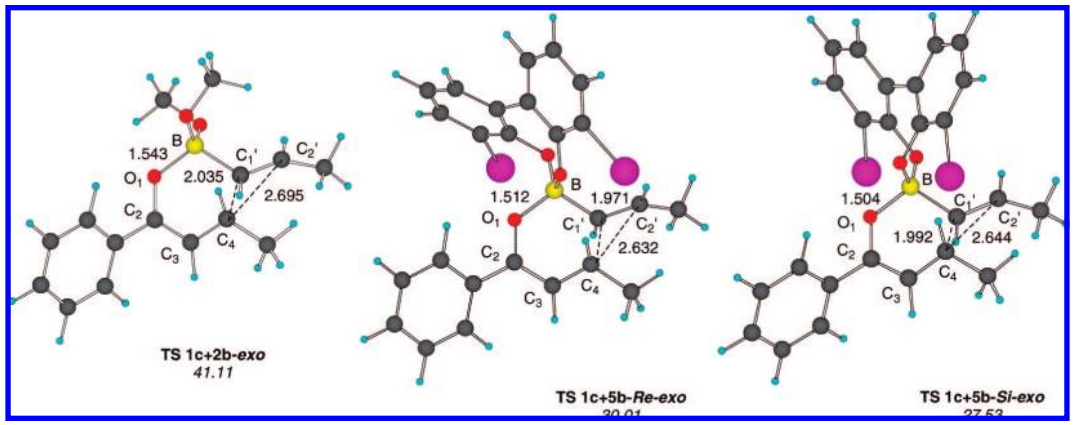

FIGURE 11. Optimized geometries for the *exo* transition structures of the 1,4-alkenylboration of **1c** with **2b** and **5b** with selected distances (in Å). Free energies relative to reactants are also shown (in italics, in kcal mol^{-1}).

SCHEME 8. Catalytic Asymmetric Conjugate Alkenylboration of Enone 1c

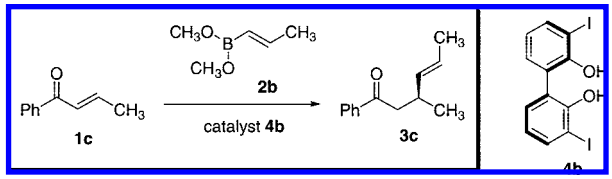

FMO analysis suggests that the reaction between the electron-rich alkenylboronate **2b** and the electron-poor ketone **1b** corresponds to an inverse electron demand hetero-Diels−Alder reaction. Conversely, the Diels−Alder reaction for the electron-deficient alkenylboronate **5b** is predicted to be a normal Diels−Alder reaction.[27] For the dimethyl alkenylboronate **2b,** classical [4 + 2] transition structures **DATSAb 1b+2b-*endo*** and ***-exo*** leading to regioisomers **10** were computed to be favored and had similar energies to the conjugate addition transition structure **TS 1b+2b-*exo*** (Figure 9). On the other hand, nonclassical [4 + 3] transition structure **DATSBa 1b+5b-*Re-endo*** corresponding to the opposite regiochemistry exhibited the lowest energy for the binaphthol-derived boronate **5b** (Figure 10). In addition, for **5b** all the Diels−Alder transition structures were computed to be less stable than their conjugate addition counterparts by more than 10 kcal mol^{-1}.

In agreement with experimental results, the hetero-Diels−Alder reactions were calculated to be kinetically disfavored relative to the conjugate alkenylboration of enone **1b** with **5b**. This is in line with our previous theoretical studies which predicted that the 1,4-alkynylboration was kinetically favored over the hetero-Diels−Alder reaction for the reaction between enones and alkynylboronates.[8] It is interesting to note, however, that

SCHEME 9. Reaction Coordinate for the 1,4-Alkenylboration of 1c with 2b Corresponding to TS 1c+2b-*exo*

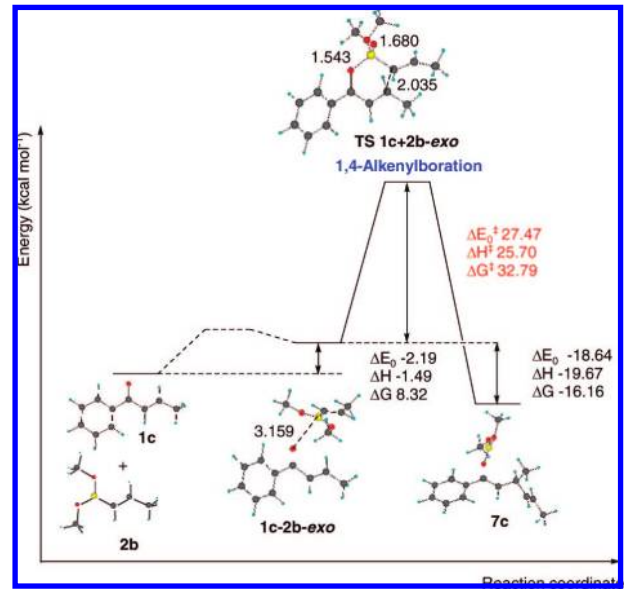

the inverse electron demand hetero-Diels−Alder reaction with the electron-rich alkenylboronate **2b** and the normal Diels−Alder reaction with the electron-deficient alkenylboronate **5b** were computed to have similar energy barriers.

Study of the Effect of Substitution on the Enone. To investigate the effect of the substitution on the vinylic position of the enone, we then studied the catalytic asymmetric conjugate addition of (*E*)-1-octenylboronate **2a** to enone **1c** catalyzed by 3,3′-diiodobinaphthol (**4a**). Enone **1c** proved to be a better substrate than enone **1b** (experimental yields: 95% vs 81%, respectively) but slightly less stereoselective (experimental er = 98.0:2.0 vs 99.1:0.9).[7] Again, we located the transition structures for the 1,4-alkenylboration reaction using **2b** and the chiral alkenylboronate derived from **4b** (**5b**) as models (Scheme 8).

Figure 11 depicts the *exo* transition structures for the conjugate alkenylboration of **1c** with **2b** and **5b**, which were calculated to be preferred over their *endo* counterparts. The geometries of the transition structures are very similar to those corresponding to enone **1b**, with B−O1 and C1′−C4 distances ca. 1.5 and 2.0 Å, respectively. The facial selectivity was also predicted to be maintained since the transition structure corre-

(25) (a) Singleton, D. A. *J. Am. Chem. Soc.* **1992**, *114*, 6563–6564. (b) Pellegrinet, S. C.; Silva, M. A.; Goodman, J. M. *J. Comput.-Aided Mol. Des.* **2004**, *18*, 209–214. (c) Pellegrinet, S. C.; Silva, M. A.; Goodman, J. M. *Tetrahedron Lett.* **2005**, *46*, 2461–2464.

(26) (a) Matteson, D. S.; Wasserbillig, J. *J. Org. Chem.* **1963**, *28*, 366–369. (b) Woods, W. G.; Bengelsdorf, I. S. *J. Org. Chem.* **1966**, *31*, 2769–2772. (c) Matteson, D. S.; Talbot, M. L. *J. Am. Chem. Soc.* **1967**, *89*, 1123–1126. (d) Evans, D. A.; Scott, W. L.; Truesdale, L. K. *Tetrahedron Lett.* **1972**, *2*, 121–124. (e) Martinez-Fresneda, P.; Vaultier, M. *Tetrahedron Lett.* **1989**, *22*, 2929–2932. (f) Rasset, C.; Vaultier, M. *Tetrahedron* **1994**, *22*, 3397–3406. (g) Bonk, J. D.; Avery, M. A. *Tetrahedron: Asymmetry* **1997**, *8*, 1149–1152. (h) Avery, M. A.; Thadani, A. N.; Lough, A. J. *J. Am. Chem. Soc.* **1999**, *121*, 450–451. (i) Avery, M. A.; Thadani, A. N.; Lough, A. J. *Chem. Commun.* **1999**, 475–476.

(27) For a study on the inverse electron demand [4 + 2] cycloadditions of alkynylboronates see: Gomez-Bengoa, E.; Helm, M. D.; Plant, A.; Harrity, J. P. A. *J. Am. Chem. Soc.* **2007**, *129*, 2691–2699.

SCHEME 10. Reaction Coordinate for the 1,4-Alkenylboration of 1c with 5b Corresponding to TS 1c+5b-*Si-exo*

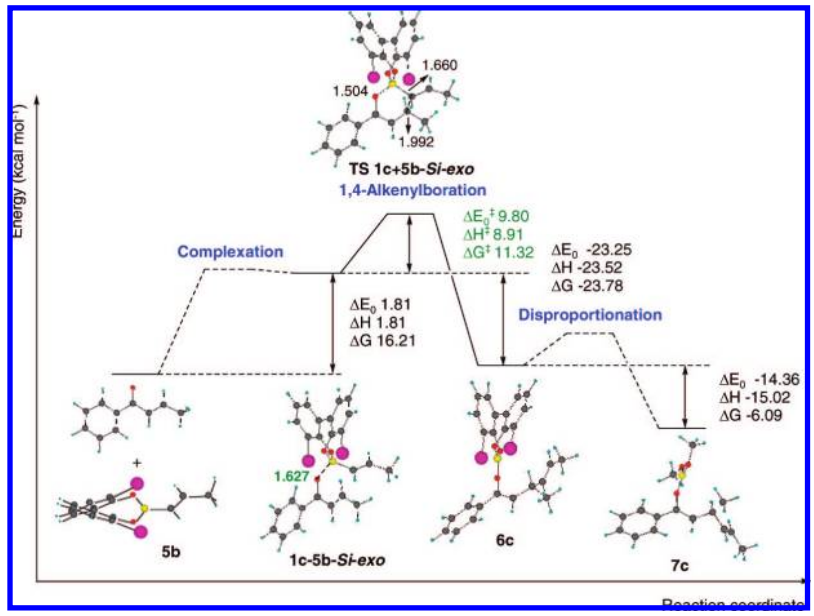

sponding to the attack of the front face (*Si* face in this case) (**TS 1c+5b-*Si-exo***) was computed to be more stable than **TS 1c+5b-*Re-exo*** by 2.48 kcal mol^{-1}. This energy difference predicts an enantiomeric ratio of 98.4:1.6 for **1c**, which is slightly lower that the one computed for enone **1b** and is in excellent agreement with the experimental value (98.0:2.0). The lower er obtained for **1c** might arise from the replacement of the phenyl in the β carbon of **1b** for a methyl, which eliminates one hydrogen−iodine close contact in the TS corresponding to the disfavored attack to the back face of the enone and thus reduces the *Re*/*Si* energy difference. In addition, the free energy barriers calculated for all transition structures for **1c** are lower than those obtained for enone **1b**. As an example, the activation free energies corresponding to the favored *exo* TSs are 27.53 vs 29.61 kcal mol^{-1} for **1c** and **1b**, respectively. This correctly reproduces the higher reactivity of α,β-unsaturated ketone **1c** observed experimentally.

The reaction profiles for the 1,4-alkenylboration of enone **1c** with **2b** and **5b** corresponding to **TS 1c+2b-*exo*** and **TS 1c+5b-*Si-exo*** are shown in Schemes 9 and 10 and resemble those of analogue **1b**. The transition structure for the reaction with alkenylboronate **2b** is connected to **1c−2b-*exo***, which shows a trigonal boron and a B−O1 distance of 3.159 Å (Scheme 9). The reaction free energy for complexation and the free energy barrier for 1,4-alkenylation were calculated to be 8.32 and 32.79 kcal mol^{-1}, respectively, which suggests the lack of reactivity of the dimethylboronate **2b**. On the other hand, transition structure **TS 1c+5b-*Si-exo*** proved to be connected to a tightly bound complex (**1c−5b-*Si-exo***) showing a tetrahedral boron atom and a boron−oxygen distance of 1.627 Å (Scheme 10). The reaction free energy for complexation is 16.21 kcal mol^{-1} while the activation free energy for the conjugate addition is 11.32 kcal mol^{-1}, making the overall process kinetically possible. Moreover, the free energy computed for the products predicts the conjugate addition step to be irreversible and thermodynamically favorable.

Study of the Effect of Substitution on the Alkenylboronate. Finally, we analyzed the effect of substitution on the alkenylboronate. We performed calculations on the model 1,4-alkenylboration reactions of enone **1c** with **2b**, **2c**, and **2d** and the

SCHEME 11. Conjugate Alkenylation of Enone 1c with Alkenylboronates 2b−d

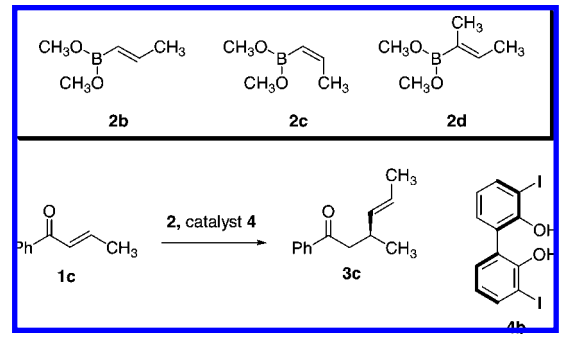

TABLE 1. Conjugate Addition of Alkenylboronates

alkenylboronate	time[a] (h)	yield[a] (%)	er[a]	calcd $\Delta G^{\ddagger}$ (kcal mol^{-1})
2b	12	92	98.7:1.3	
			calcd 98.4:1.6	*Re-exo* 30.01
				Si-exo 27.53
2c	18	91	95.5:4.5	
			calcd 98.6:1.4	*Re-endo*29.00
				Si-exo 26.40
2d	36	57	65:35	
			calcd 86.7:13.3	*Re-exo* 31.32
				Si-exo 30.20

[a] Experimental results for chalcone (**1a**) and dimethyl (*E*)- and (*Z*)-1-octenyl and (*E*)-1-ethylbutenyl boronates catalyzed by 3,3′-diiodobinaphthol (**4a**).

corresponding alkenylboronates derived from biphenol **4b** (Scheme 11, Table 1). We then compared the results with the data obtained experimentally for the reaction of chalcone (**1a**, Scheme 1) with the monosubstituted (*E*)- and (*Z*)-1-octenylboronates and the 1,2-disubstituted (*E*)-1-ethylbutenylboronate catalyzed by 3,3′-diiodobinaphthol (**4a**).[7]

The observed reactivities decreased in the order (*E*)- > (*Z*)- > 1,2-disubstituted alkenylboronate and the stereoselectivity followed the same trend (Table 1). Calculations predicted the lower reactivity and selectivity of the 1,2-disubstituted alkenylboronate **2d**, although the er was overestimated. In addition,

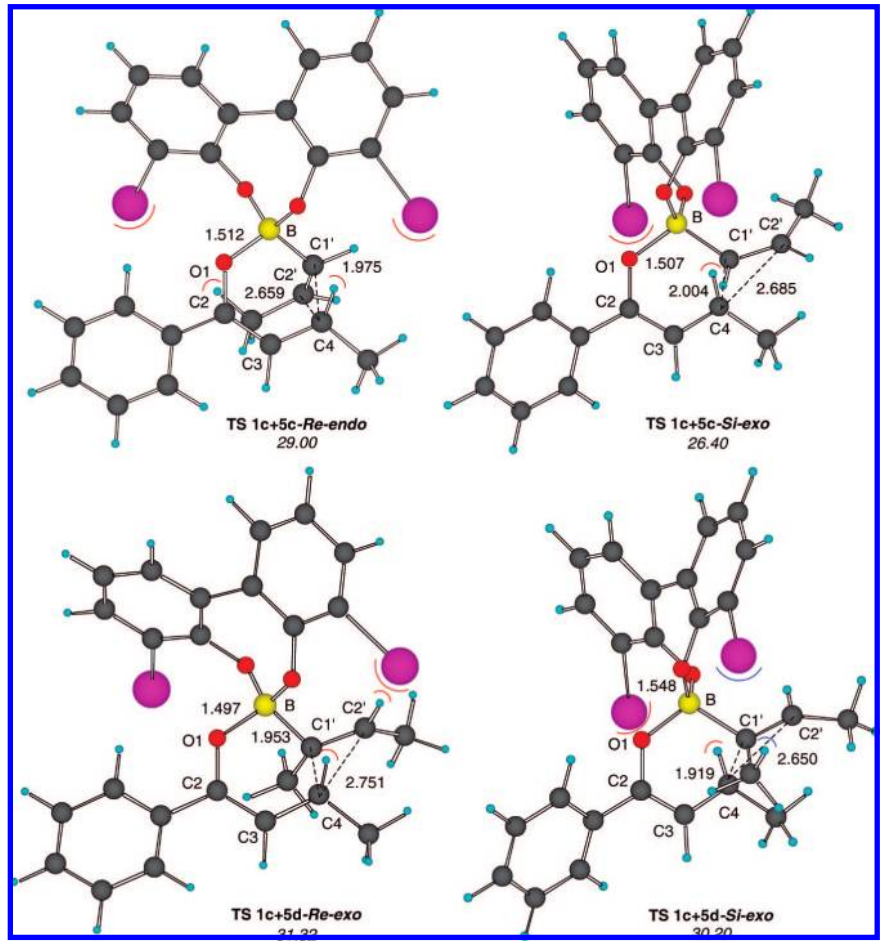

FIGURE 12. Optimized geometries for the more favorable *Re* and *Si* transition structures of the 1,4-alkenylboration of **1c** with **5c** and **5d** with selected distances (in Å). Free energies relative to reactants are also shown (in italics, in kcal mol^{-1}). The lowest energy transition structure closely resembles the model given in Scheme 5.

SCHEME 12. Reaction Coordinate for the 1,4-Alkenylboration of 1c with 5b−d Corresponding to the *Si-exo* TS and Free Energies for 5b−d from Top to Bottom

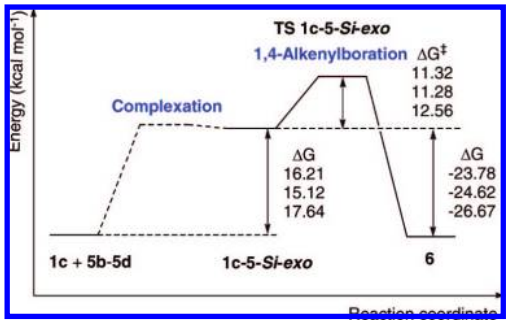

the reactivity and stereoselectivity computed for **2c** were slightly higher than the ones obtained for **2b**. These subtle discrepancies with the experimental results might be due to the fact that models were used to perform the calculations. However, reactivity and selectivity trends were nicely reproduced.[28]

(28) We performed similar calculations to study the effect of substitution on the alkenylboronate using binaphthol instead of 3,3′-diodobiphenol (**4b**) as a model for 3,3′-diiodobinaphthol (**4a**). The computed reactivity for **2b** and **2c** was nearly the same and slightly lower than that for **2d**, while the enantiomeric ratios were ca. 99:1 for **2b** and **2d** and 98:2 for **2c**, so model **4b** predicts ratios that are closer to those obtained experimentally. These results might suggest that binaphthol could be a better ligand for the conjugate addition of 1,2-disubstituted alkenylboronates.

The optimized geometries for the more favorable *Re* and *Si* transition structures of the 1,4-alkenylboration of **1c** with **5c** and **5d** are shown in Figure 12.

The *Si* facial selectivity observed with these systems can be rationalized by considering the two close contacts experienced between the iodine atoms in the ligands and two hydrogens in the *Re* TSs. **TS 1c+5b-*Si-exo*** (Figure 11) and **TS 1c+5c-*Si-exo*** show only one close contact between C4−H and one of the iodines. On the other hand, the presence of a methyl group in C1′ of alkenylboronate **5d** generates an extra close contact with the other iodine atom in **TS 1c+5d-*Si-exo*** (shown in blue) so the activation energy increases and the energy difference with its *Re* counterpart decreases. QRC calculations[15] for the favored *Si-exo* TSs in the conjugate addition of alkenylboronates **5b**, **5c**, and **5d** to enone **1c** also suggest that both the initial complexation and the 1,4-alkenylation step are more energy demanding for the 1,2-disubstituted derivative (**5d**) (Scheme 12).

Conclusions

The mechanism of the asymmetric conjugate addition of alkenylboronates to enones catalyzed by binaphthols has been studied with DFT methods. On the basis of the structures and energies for a model reaction, a revised key transition state for the catalytic cycle was proposed, going through a sofalike and not a chairlike conformation. Initial exchange of methoxy ligands gives the chiral and highly Lewis acidic alkenylboronate, which under-

goes reversible complexation with the enone. Subsequent fast and irreversible intramolecular conjugate addition yields a boron enolate product that finally disproportionates with the dimethylboronate, releasing the chiral alkenylboronate for further reaction. FMO theory has been used to account for the greater reactivity of the binaphthol-derived alkenylboronate. Furthermore, the boron atom of the alkenylboronate and the enone moiety were found to be in the same plane in all the 1,4-alkenylboration transition structures, so the key asymmetric step goes through a sofalike transition structure. In addition, competitive reactions, such as hetero-Diels−Alder reactions, were shown to be kinetically disfavored. Experimental results for various enones and alkenylboronates were nicely reproduced and the factors affecting the reactivities and stereoselectivities were also assessed.

Acknowledgment. We thank CONICET, Universidad Nacional de Rosario and ANPCyT (SCP), EPSRC, and St. Catharine's College for a Research Fellowship (RSP) and Unilever.

Supporting Information Available: Activation energies including zero-point energy (ZPE) corrections, activation enthalpies, activation free energies, and activation free energies in solution for all the reactions of enone **1b**; Cartesian coordinates, absolute energies including ZPE (in hartrees) and number of imaginary frequencies of all the stationary points reported in the paper; free energies in solution of selected structures; values of imaginary frequencies of all transition structures; optimized geometries of key structures not included in the paper; and energies of the frontier molecular orbitals of the reactants not included in the paper (in eV). This material is available free of charge via the Internet at http://pubs.acs.org.

JO8007463